

# $\alpha$ -particle photoabsorption with a realistic nuclear force

Doron Gazit<sup>1</sup>, Sonia Bacca<sup>2</sup>, Nir Barnea<sup>1</sup>,

Winfried Leidemann<sup>3</sup>, and Giuseppina Orlandini<sup>3</sup>

<sup>1</sup>*The Racah Institute of Physics, The Hebrew University, 91904 Jerusalem, Israel*

<sup>2</sup>*Gesellschaft für Schwerionenforschung,*

*Planckstr. 1, 64291 Darmstadt, Germany and*

<sup>3</sup>*Dipartimento di Fisica, Università di Trento and Istituto Nazionale di Fisica Nucleare,*

*Gruppo Collegato di Trento, I-38050 Povo, Italy*

(Dated: February 5, 2020)

## Abstract

The  $^4\text{He}$  total photoabsorption cross section is calculated with the realistic nucleon-nucleon potential Argonne V18 and the three-nucleon force (3NF) Urbana IX. Final state interaction is included rigorously via the Lorentz Integral Transform method. A rather pronounced giant resonance with peak cross sections of 3 (3.2) mb is obtained with (without) 3NF. Above 50 MeV strong 3NF effects, up to 35%, are present. Good agreement with experiment is found close to threshold. A comparison in the giant resonance region is inconclusive, since present data do not show a unique picture.

PACS numbers: 21.45.+v, 21.30.Fe, 25.20.Dc, 24.30.Cz

In the last three decades there has been a continuous interest in  $^4\text{He}$  photodisintegration, both in theory and in experiment (see [1, 2] and references therein). The  $\alpha$ -particle is drawing such a great attention because it has some typical features of heavier systems (e.g. binding energy per nucleon), which make it an important link between the classical few-body systems, i.e. deuteron, triton and  $^3\text{He}$ , and more complex nuclei. For example in  $^4\text{He}$  one can study the possible emergence of collective phenomena typical of complex nuclei like the giant resonance. Furthermore  $^4\text{He}$  is the ideal testing ground for microscopic two- and three-body forces, which are fitted in the two- and three-body systems. At present the 3NF is not yet well determined, thus it is essential to search for observables where it plays an important role. Because of gauge invariance, in electromagnetic processes nuclear forces manifest themselves also as exchange currents, which have turned out to be very important in photonuclear reactions and hence 3NF effects might become significant. For the three-nucleon systems photonuclear processes have already been studied [3, 4, 5], e.g. in [3] it was found that the 3NF leads to an almost 10% reduction of the electric dipole peak and up to 15% enhancement at higher energy. One expects that the 3NF is of considerably greater relevance in the four-body system, since there one has six nucleon pairs and four triplets, compared to three pairs and just one triplet in the three-nucleon systems.

Unfortunately, the current theoretical and experimental situation of the  $^4\text{He}$  photodisintegration is not sufficiently settled. Most of the experimental work has concentrated on the two-body break-up channels  $^4\text{He}(\gamma, n)^3\text{He}$  and  $^4\text{He}(\gamma, p)^3\text{H}$  in the giant resonance region, but still today there is large disagreement in the peak. In fact in two very recent  $(\gamma, n)$  experiments [1, 2] one finds differences of a factor of two. The  $^4\text{He}(\gamma)$  reaction represents a very challenging theoretical problem as well, since the full four-body continuum dynamics and all possible fragmentations have to be considered. Calculations with realistic nuclear forces have not yet been carried out. Even investigations with a realistic nucleon-nucleon (NN) interaction and without a 3NF are still missing. Calculations exist only for semi-realistic NN potentials. In Refs. [6, 7, 8] it has been shown that such models lead to pronounced peak cross sections, in rather good agreement with the experimental data of [1] and much different from what was calculated earlier [9].

It is evident that the experimental and theoretical situations are very unsatisfactory. With the present work we make an important step forward on the theory side performing a calculation of the  $\alpha$ -particle total photoabsorption cross section with a realistic nuclear

force. To this end we solve the four-body problem taking as nuclear interaction the realistic Argonne V18 (AV18) NN potential [11] and the Urbana IX (UIX) 3NF [12]. We reduce the continuum state problem to a bound-state like problem via the Lorentz Integral Transform (LIT) method [10], thus taking into account the full final state interaction rigorously. The LIT bound-state like problem, as well as that of the  ${}^4\text{He}$  ground state, is solved via expansions in hyperspherical harmonics (HH) using the powerful effective interaction HH (EIHH) approach [13, 14]. The reliability of the EIHH technique in electromagnetic processes with the AV18 and UIX potentials has been shown in a recent  ${}^3\text{H}(\gamma)$  calculation [15].

We calculate the total photoabsorption cross section  $\sigma_\gamma(\omega)$  in the unretarded dipole approximation. In this way the dominant part of the exchange current contribution on the total cross section is taken into account via the Siegert theorem. In the classical few-body systems it has been found [4, 16] that this is an excellent approximation, particularly for photon energies  $\omega$  below 50 MeV. For example for the triton  $\sigma_\gamma(\omega)$  the contributions of retardation and all other multipoles lead to a cross section enhancement of less than 1% for  $\omega \leq 40$  MeV and of 5 (5)%, 16 (18)%, and 26 (33)% with AV18 (AV18+UIX) at  $\omega = 60, 100, \text{ and } 140$  MeV, respectively [4].

The total photoabsorption cross section is given by

$$\sigma_\gamma(\omega) = 4\pi^2\alpha\omega R(\omega), \quad (1)$$

where  $\alpha$  is the fine structure constant and

$$R(\omega) = \int d\Psi_f \left| \langle \Psi_f | \hat{D}_z | \Psi_0 \rangle \right|^2 \delta(E_f - E_0 - \omega) \quad (2)$$

is the response function in the unretarded dipole approximation with  $\hat{D}_z = \sum_{i=1}^A \frac{\tau_i^3 z'_i}{2}$ . The wave functions of the ground and final states are denoted by  $|\Psi_{0/f}\rangle$  and the energies by  $E_{0/f}$ , respectively. The operators  $\tau_i^3$  and  $z'_i$  are the third components of the  $i$ -th nucleon isospin and center of mass frame position. In the LIT method one obtains  $R(\omega)$  from the inversion of an integral transform with a Lorentzian kernel [10]

$$L(\sigma_R, \sigma_I) = \int d\omega \frac{R(\omega)}{(\omega - \sigma_R)^2 + \sigma_I^2} = \langle \tilde{\Psi} | \tilde{\Psi} \rangle, \quad (3)$$

where  $\tilde{\Psi}$  is the unique solution of an inhomogeneous ‘‘Schrödinger-like’’ equation

$$(H - E_0 - \sigma_R + i\sigma_I) |\tilde{\Psi}\rangle = \hat{D}_z |\Psi_0\rangle \quad (4)$$

with bound-state like asymptotic boundary conditions.

The EIHH expansions of  $\Psi_0$  and  $\tilde{\Psi}$  are performed with the full HH set up to maximal values of the HH grand-angular momentum quantum number  $K$  ( $K \leq K_m^0$  for  $\Psi_0$ ,  $K \leq K_m$  for  $\tilde{\Psi}$ ). The convergence of binding energy and matter radius are presented in Table I. Our final binding energy results of 24.27 MeV (AV18) and 28.42 MeV (AV18+URBIX) agree quite well with other calculations (AV18: 24.25 [17], 24.22 [18], 24.21 [19] MeV); AV18+URBIX: 28.34 [20], 28.50 [17], 28.46 [19] MeV).

The EIHH convergence of the transform  $L$  is excellent for the AV18 potential. Here we discuss in detail only the case AV18+UIX, where the convergence is quite good, but not at such an excellent level. The reason is that in our present EIHH calculation an effective interaction is constructed only for the NN potential, while the 3NF is taken into account as bare interaction. In Fig. 1 we show results for the transform  $L$  obtained with various  $K_m$  and  $K_m^0$ . Since we take  $K_m^0 = K_m - 1$  the corresponding transform can be denoted by  $L_{K_m}$ . One sees that there is a very good convergence beyond the peak. The figure also shows that the peak height is very well established, but that the peak position is not yet completely converged. In fact with increasing  $K_m$  the peak is slightly shifted towards lower  $\sigma_R$ . This is illustrated better in Fig. 2, where we show the relative differences  $\Delta_{K_m} = L_{K_m,19}/L_{19}$  with  $L_{\alpha,\beta} = L_\alpha - L_\beta$  (the chosen  $\sigma_R$ -range starts at the  ${}^4\text{He}(\gamma)$  break-up threshold). One again notes the very good convergence for  $\sigma_R > 30$  MeV with almost identical results from  $L_{13}$  to  $L_{19}$ . Altogether we consider our result for  $\sigma_R > 30$  MeV as completely sufficient. On the other hand it is obvious that convergence is not entirely reached for lower  $\sigma_R$ . Here we should mention that for  $L_{19}$  there are already 364000 states in the HH expansion. A further increase is beyond our present computational capabilities. On the other hand, as a closer inspection of Fig. 2 shows, the convergence proceeds with a rather regular pattern: (i)  $L_{13,11} \simeq L_{11,9}$  and  $L_{17,15} \simeq L_{15,13}$  and (ii)  $L_{19,17} \simeq L_{17,15}/1.5 \simeq L_{13,11}/(1.5)^2$ . Due to this regular pattern it is possible to obtain an extrapolated asymptotic result. We use the following Padé approximation

$$L_{K_m}^\infty = L_{K_m-8} + L_{K_m-4,K_m-8}/\left(1 - \frac{L_{K_m,K_m-4}}{L_{K_m-4,K_m-8}}\right). \quad (5)$$

In Fig. 3 we illustrate the results for  $\sigma_{\gamma,K_m}$  obtained from the inversions of the corresponding transforms  $L_{K_m}$ . Due to the Lorentz kernel the cross section presents the same features as  $L$  itself: established peak height with a value very close to 3 mb, and not yet completely

convergent peak position. In Fig. 3 we also show  $\sigma_{\gamma,17}^\infty$  and  $\sigma_{\gamma,19}^\infty$  resulting from the inversion of  $L_{17}^\infty$  and  $L_{19}^\infty$ , respectively. Unquestionably, the extrapolated  $L_{K_m}^\infty$  have a lower numerical quality than the calculated  $L_{K_m}$  and consequently we do not find the same stability for the corresponding inversions (for details on inversion see [21]). Therefore we use an additional constraint in the inversion by fixing the peak cross section to the already converged value of 3 mb. In Fig. 3 it is evident that  $\sigma_{\gamma,17}^\infty$  and  $\sigma_{\gamma,19}^\infty$  are very similar, hence establishing a very good approximation for the asymptotic  $\sigma_\gamma$ . One also notices that compared to  $\sigma_{\gamma,19}$  they show a shift of the peak position by about 1 MeV towards lower energy.

In Fig. 4a we show our final results for  $\sigma_\gamma$ . Due to the 3NF one observes a reduction of the peak height by about 6% and a shift of the peak position by about 1 MeV towards higher energy. Very large effects of the 3NF are found above 50 MeV with an enhancement of  $\sigma_\gamma$  by e.g. 18, 25, and 35% at  $\omega = 60, 100,$  and  $140$  MeV, respectively (3NF effect could change somewhat if all multipole contributions are considered, see also discussion before Eq. (1)). The comparison between the present results and those obtained with semi-realistic potential models [6, 7] is similar as in the three-nucleon photodisintegration [3]: semi-realistic models lead to rather realistic results in the giant resonance region overestimating the peak by about 10-15% and giving quite a correct result for the the peak position; however, at higher  $\omega$  the cross section is strongly underestimated (in the present case by a factor of three at pion threshold).

It is very interesting to compare the 3NF effects on  $\sigma_\gamma$  to those found in the three-body nuclei [3, 4]. Surprisingly, the reduction of the  ${}^4\text{He}$  peak height is smaller than in the three-nucleon case. For  ${}^3\text{H}/{}^3\text{He}$  its size is similar to the binding energy increase (10%), whereas for  ${}^4\text{He}$  the 3NF increases the binding energy by 17%, but reduces the peak by only 6% and thus cannot be interpreted as a simple binding effect. Also at higher  $\omega$  there are important differences. The enhancement of the  ${}^4\text{He}$  cross section due to the 3NF is significantly higher, namely about two times larger than for the three-body case. Interestingly this reflects the above mentioned different ratios between triplets and pairs in three- and four-body systems.

In Fig. 4b we compare our results to experimental data. For the AV18+UIX case upper/lower bounds are included to account for possible errors in the extrapolation (5). The bounds are obtained enhancing/reducing the difference  $\sigma_{\gamma,19}^\infty - \sigma_{\gamma,19}$  by 50%; we believe that this is a rather safe error estimate. The data in Fig. 4b have to be interpreted with some care: (i) in [22] the peak cross section is determined from Compton scattering via dispersion

relations, (ii) the dashed area corresponds to the sum of cross sections for  $(\gamma, n)$  from [23] and  $(\gamma, p)^3\text{H}$  from [24] as already shown in [6], (iii) the data from the above mentioned recent  $(\gamma, n)$  experiment [1] are included only up to about the three-body break-up threshold, where one can rather safely assume that  $\sigma_\gamma \simeq 2\sigma(\gamma, n)$  (see also [8]), (iv) in [2] all open channels are considered. One sees that the various data are quite different exhibiting maximal deviations of about a factor of two. The theoretical  $\sigma_\gamma$  agrees quite well with the low-energy data of [23, 24]. In the peak region, however, the situation is very unclear. There is a rather good agreement between the theoretical  $\sigma_\gamma$  and the data of [1] and [22], while those of [23, 24] are noticeably lower. Very large discrepancies are found in comparison to the recent data of Shima et al. [2]. It is evident that the experimental situation is rather unsatisfactory and further improvement is urgently needed.

We summarize our work as follows. We have performed an ab initio calculation of the  $^4\text{He}$  total photoabsorption cross section using a realistic nuclear force (AV18 NN potential plus the UIX-3NF). The full interaction is consistently taken into account both in the ground state and in the continuum via the LIT method. For the solutions of the differential equations we use expansions in hyperspherical harmonics via the EIH approach. Our results show a rather pronounced giant dipole peak. The 3NF reduces the peak height by only about 6%, less than expected considering its large effect of almost 20% on the  $^4\text{He}$  binding energy and its different role in the three-nucleon system. Beyond the giant dipole resonance 3NF effects become much larger. With growing  $\omega$  their importance increases and at pion threshold one has an enhancement of 35%, about twice the effect one finds in  $^3\text{H}/^3\text{He}$  photoabsorption. Close to threshold the theoretical cross section agrees quite well with experimental data. In the giant resonance region, where there is no established experimental cross section, our results are in good agreement with the data of [1] and [22], while we find a strong disagreement with the data of [2].

In conclusion we would like to emphasize that it is very important to understand whether a nuclear force model, which is constructed in the two- and three-nucleon systems, is sufficient to explain the four-nucleon photodisintegration. To this end further experimental investigations are mandatory.

This work was supported by the Israel Science Foundation (grant no 202/02) and by the Italian Ministry of Research (COFIN03). Numerical calculations were partly performed at

CINECA (Bologna); one of us (S.B.) thanks S. Boschi (CINECA) for his professional help.

---

- [1] B. Nilsson et al., Phys. Lett. B **626**, 65 (2005).
- [2] T. Shima, S. Naito, Y. Nagai, T. Baba, K. Tamura, T. Takahashi, T. Kii, H. Ohgaki, and H. Toyokawa, Phys. Rev. C **72**, 044004 (2005).
- [3] V.D. Efros, W. Leidemann, G. Orlandini, and E.L. Tomusiak, Phys. Lett. B **484**, 223 (2000).
- [4] J. Golak, R. Skibiński, W. Glöckle, H. Kamada, A. Nogga, H. Wiśniewski, V.D. Efros, W. Leidemann, G. Orlandini, and E.L. Tomusiak, Nucl. Phys. A **707**, 365 (2002).
- [5] J. Golak, R. Skibiński, H. Wiśniewski, W. Glöckle, A. Nogga, and H. Kamada, Phys. Rep. **415**, 89 (2005).
- [6] V.D. Efros, W. Leidemann, and G. Orlandini, Phys. Rev. Lett. **78**, 4015 (1997).
- [7] N. Barnea, V.D. Efros, W. Leidemann, and G. Orlandini, Phys. Rev. C **63**, 057002 (2001).
- [8] S. Quaglioni, W. Leidemann, G. Orlandini, N. Barnea, and V.D. Efros, Phys. Rev. C **69**, 044002 (2004).
- [9] G. Ellerkmann, W. Sandhas, S.A. Sofianos, and H. Fiedeldey, Phys. Rev. C **53**, 2638 (1996).
- [10] V.D. Efros, W. Leidemann, and G. Orlandini, Phys. Lett. B **338**, 130 (1994).
- [11] R.B. Wiringa, V.G.J. Stoks, and R. Schiavilla, Phys. Rev. C **51**, 38 (1995).
- [12] B.S. Pudliner, V.R. Pandharipande, J. Carlson, S.C. Pieper, and R.B. Wiringa, Phys. Rev. C **56**, 1720 (1997).
- [13] N. Barnea, W. Leidemann, and G. Orlandini, Phys. Rev. C **61**, 054001 (2000); Nucl. Phys. A **693**, 565 (2001).
- [14] N. Barnea, V.D. Efros, W. Leidemann, and G. Orlandini, Few-Body Syst. **35**, 155 (2004).
- [15] N. Barnea, W. Leidemann, G. Orlandini, V.D. Efros, and E.L. Tomusiak, nucl-th/0511075.
- [16] H. Arenhövel and M. Sanzone, Few-Body Syst. Suppl. **3**, 1 (1991).
- [17] A. Nogga, H. Kamada, W. Glöckle, and B.R. Barrett, Phys. Rev. C **65**, 054003 (2002).
- [18] R. Lazauskas and J. Carbonell, Phys. Rev. C **70**, 044002 (2004).
- [19] M. Viviani, A. Kievsky, and S. Rosati, Phys. Rev. C **71**, 024006 (2005).
- [20] R.B. Wiringa, S.C. Pieper, J. Carlson, and V.R. Pandharipande, Phys. Rev. C **62**, 014001 (2000).
- [21] V.D. Efros, W. Leidemann, and G. Orlandini, Few-Body Syst. **26** (1999) 251.

- [22] D.P. Wells, D.S. Dale, R.A. Eisenstein, F.J. Federspiel, M.A. Lucas, K.E. Mellendorf, A.M. Nathan, and A.E. O'Neill , Phys. Rev. C **46**, 449 (1992).
- [23] B.L. Berman, D.D. Faul, P. Meyer, and D.L. Olson, Phys. Rev. C **22**, 2273 (1980).
- [24] G. Feldman, M.J. Balbes, L.H. Kramer, J.Z. Williams, H.R. Weller, and D.R. Tilley, Phys. Rev. C **42**, R1167 (1990).



Fig. 1

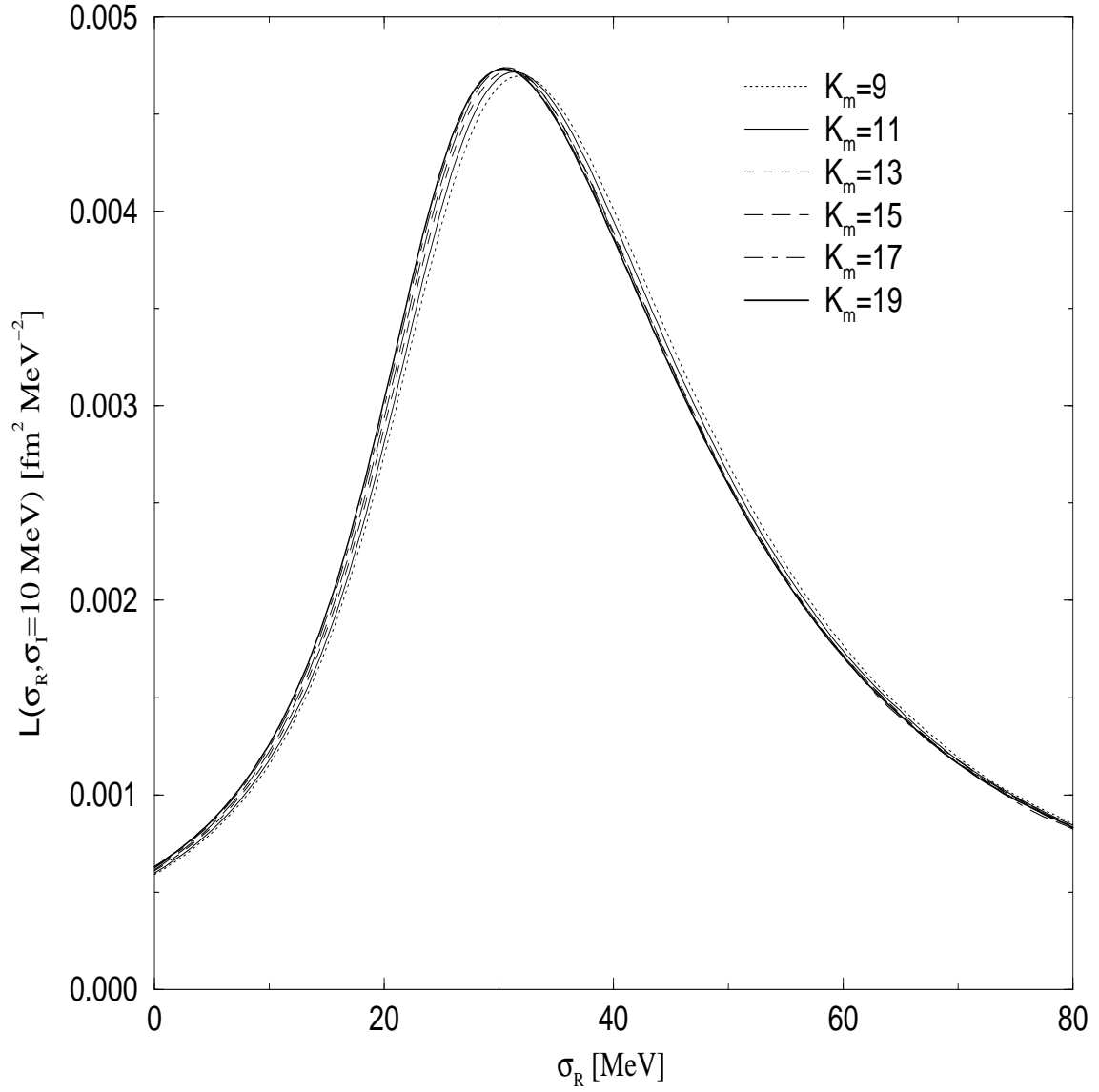


FIG. 1: Convergence of  $L_{K_m}$  with  $\sigma_I = 10$  MeV (AV18+UIX).

Fig. 2

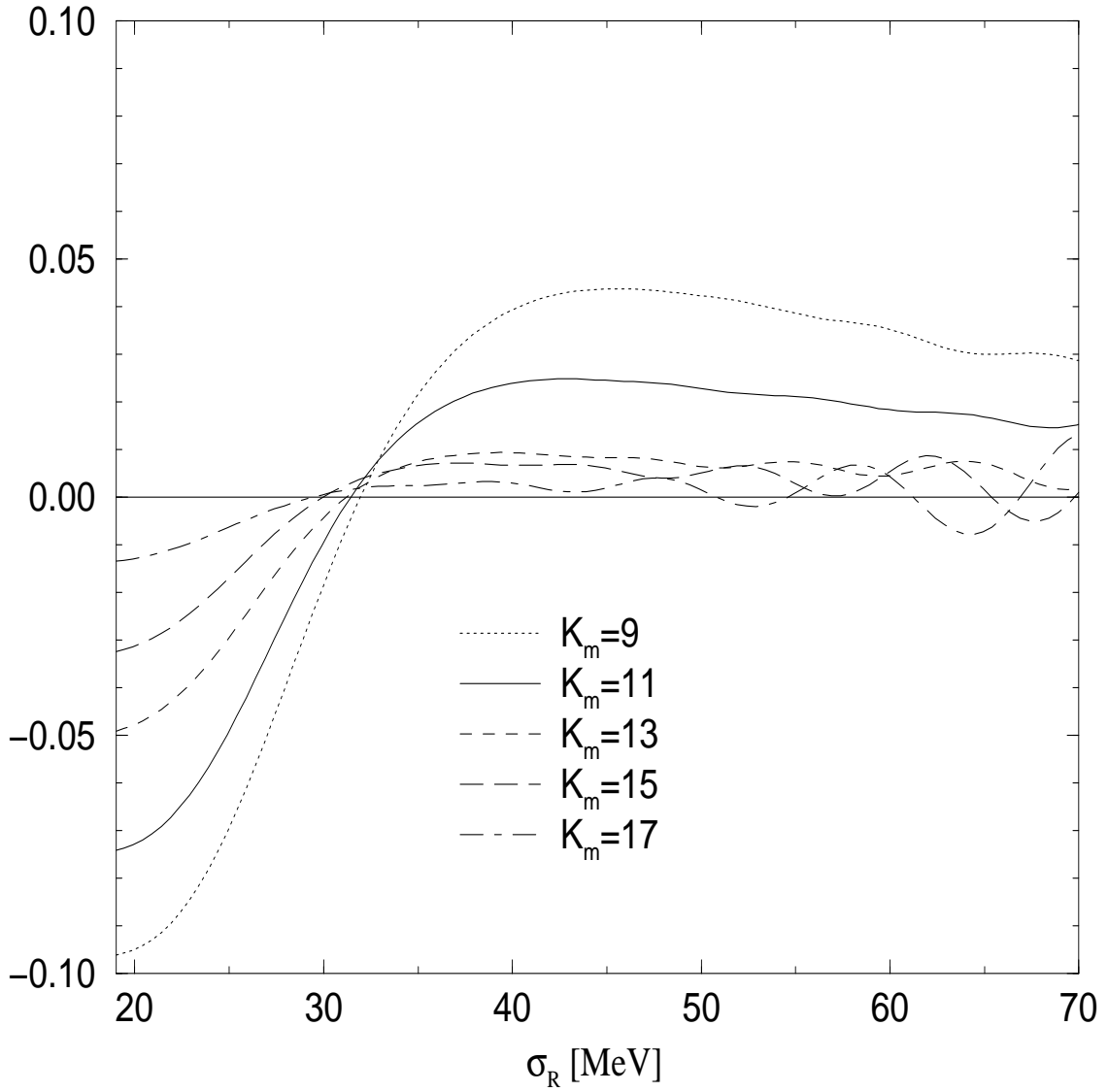


FIG. 2: Convergence of  $\Delta_{K_m} = (L_{K_m} - L_{19})/L_{19}$  (AV18+UIX).

Fig. 3

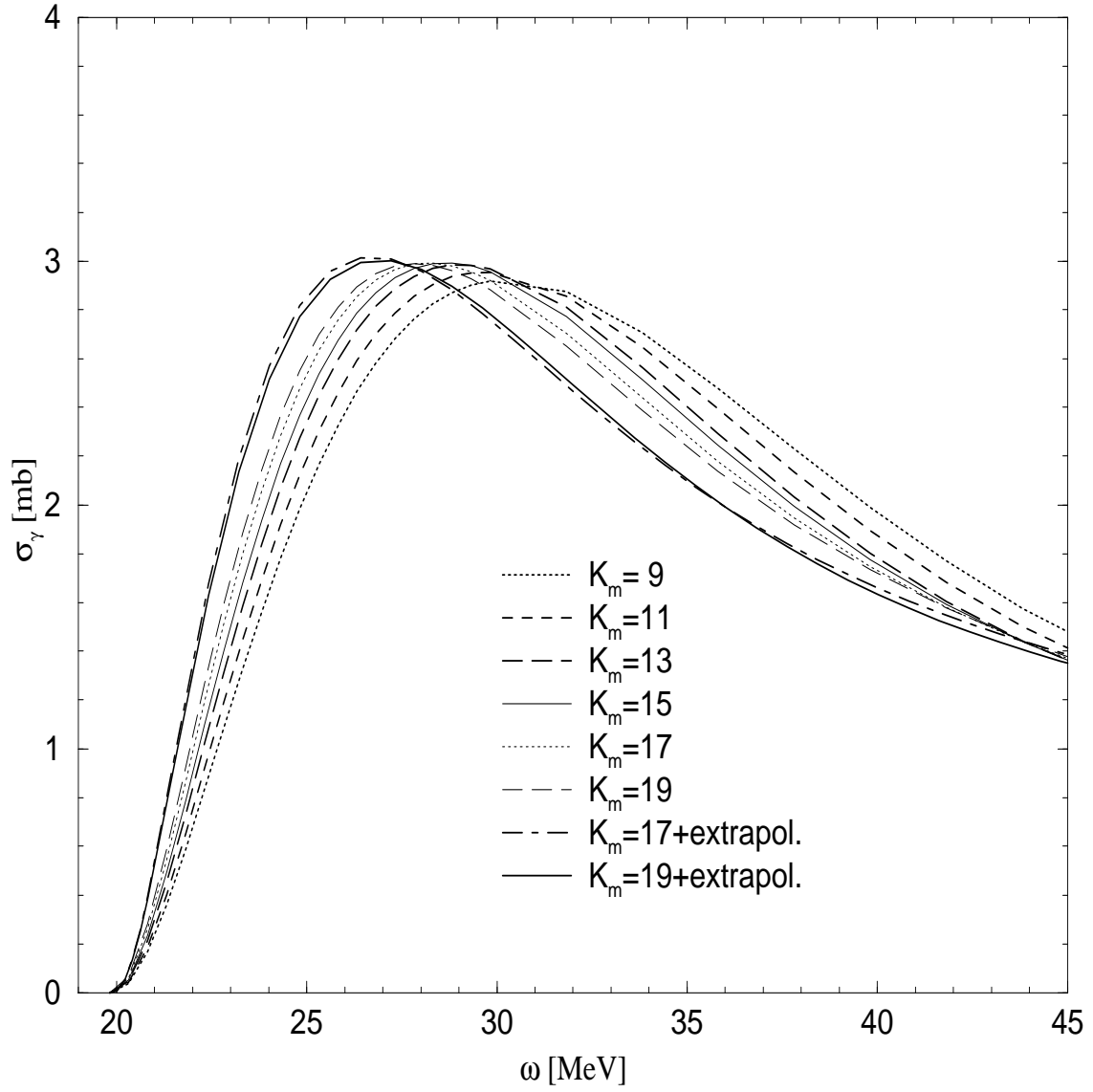


FIG. 3: Convergence of  $\sigma_{\gamma,K_m}$  (AV18+UIX), also shown  $\sigma_{\gamma,17}^\infty$  and  $\sigma_{\gamma,19}^\infty$ .

Fig. 4

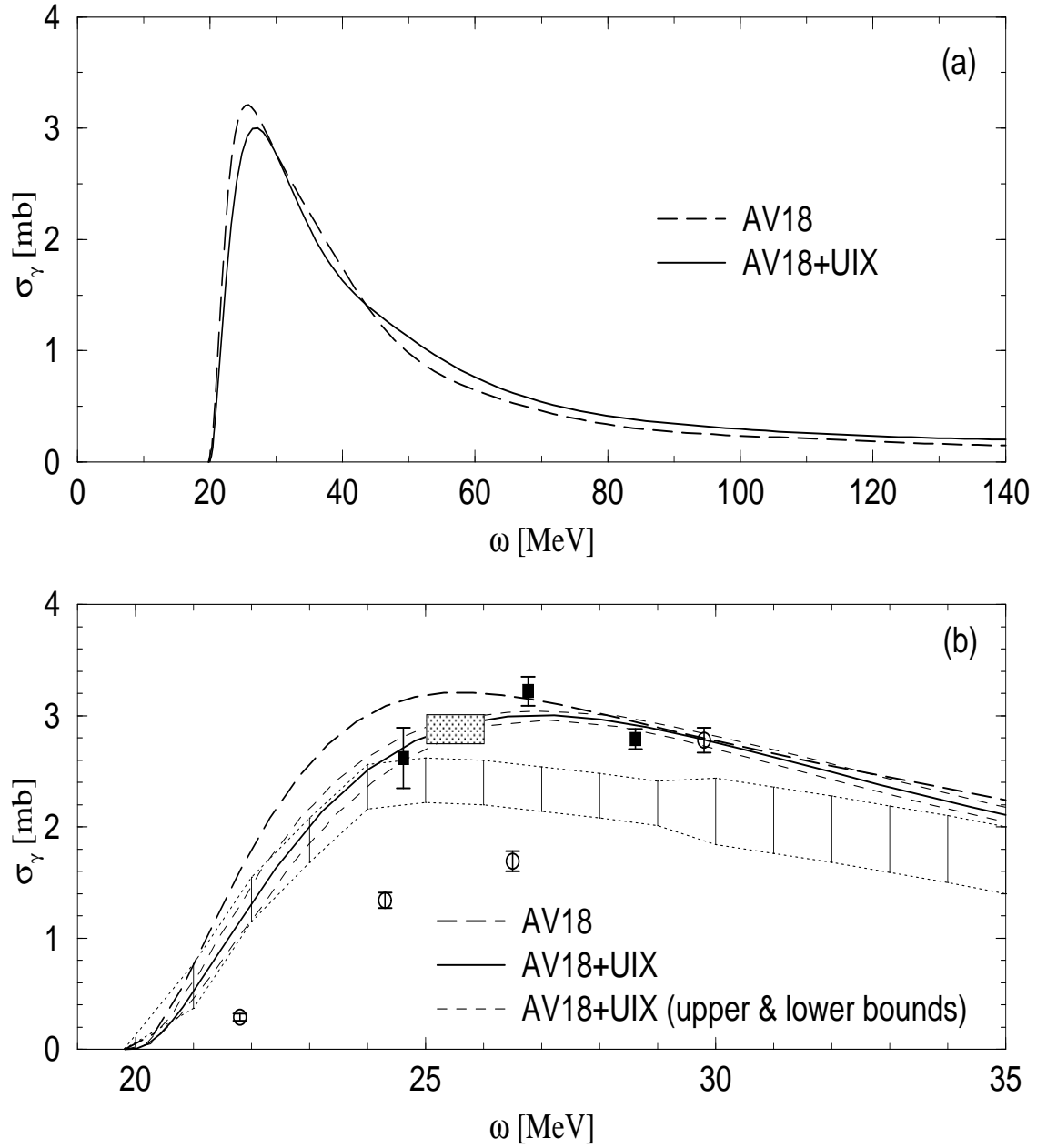


FIG. 4: Total  ${}^4\text{He}$  photoabsorption cross section: (a)  $\sigma_\gamma$  (AV18) and  $\sigma_{\gamma,19}^\infty$  (AV18+UIX), (b) as (a) but also included upper/lower bounds and various experimental data (see text), area between dotted lines [23, 24], dotted box [22], squares [1], and circles [2].

TABLE I: Convergence of HH expansion for  ${}^4\text{He}$  binding energy  $E_b$  [MeV] and root mean square matter radius  $\langle r^2 \rangle^{\frac{1}{2}}$  [fm] with AV18 and AV18+UIX potentials.

$K_m^0$	AV18		AV18+UIX	
	$E_b$	$\langle r^2 \rangle^{\frac{1}{2}}$	$E_b$	$\langle r^2 \rangle^{\frac{1}{2}}$
6	25.312	1.506	26.23	1.456
8	25.000	1.509	27.63	1.428
10	24.443	1.520	27.861	1.428
12	24.492	1.518	28.261	1.427
14	24.350	1.518	28.324	1.428
16	24.315	1.518	28.397	1.430
18	24.273	1.518	28.396	1.431
20	24.268	1.518	28.418	1.432